Influence of bismuth on the corrosion of lead in 5 M H_2SO_4

M. J. Koop and **D. F. A. Koch**
Department of Chemical Engineering, Monash University, Clayton, Vic. 3168 (Australia)

D. A. J. Rand*
CSIRO, Division of Mineral Products, P.O. Box 124, Port Melbourne, Vic. 3207 (Australia)

(Received December 20, 1990)

Abstract

Bismuth exerts a dual influence on the corrosion of lead beneath the $PbSO_4$ film that is formed on the metal at applied potentials in sulphuric acid solution. First, by altering the morphology of the $PbSO_4$ crystals, bismuth (either alloyed with the metal, or dissolved in the acid) causes the development of a more porous film that promotes an increased attack of the underlying substrate. Second, bismuth modifies the grain structure of lead and this, in turn, determines the extent of corrosion under the $PbSO_4$ film.

Introduction

There has been considerable debate over whether bismuth exerts a beneficial or a deleterious effect on the performance of lead/acid batteries. Resolution of this problem is important to both metal suppliers and battery manufacturers alike — bismuth is a naturally occurring minor element in a number of lead ores and its removal is both irksome and costly. There is, therefore, strong commercial pressure to establish a maximum tolerable level for bismuth in the raw lead materials employed in battery production.

Bismuth can enter a lead/acid battery either via the leady oxide used in the preparation of the plate active-material [1], or via the grid alloy. Very little information has been published concerning the possible influence of leady-oxide-based bismuth on the ease-of-processing and quality of the oxide itself, the resulting paste characteristics, or the eventual performance of the battery. There are undocumented claims within the industry that the presence of bismuth causes 'stickiness' of the oxide and thus impairs handleability. Nevertheless, Agruss *et al.* [2] found that the capacity, deep-cycle endurance and shelf-life of batteries were all unaffected by bismuth concentrations of up to 0.25 wt.% in the starting oxide.

*Author to whom correspondence should be addressed.

0378-7753/91/$3.50

Greater attention has been directed towards the behaviour of bismuth when contained in the grid alloy. Devitt and Myers [3] showed that batteries using grids with bismuth contents in the range 0.0007 to 0.042 wt.% exhibited no ill effects under the SAE J537 overcharge life test, a schedule that is designed to cause battery failure by grid corrosion. By contrast, cycle life tended to increase with increasing bismuth content when batteries were subjected to the SAE J240 test, a procedure that aims to simulate duty in an automobile. Hoehne [4, 5] found that the presence of bismuth (0.006 to 0.2 wt.%) both encouraged the shedding of positive-plate material and promoted the growth of grids. The progressive changes in the extent of these phenomena were not, however, linear with increasing bismuth content. For example, grid growth was virtually the same at 0.006 and 0.075 wt.% Bi, but doubled at 0.2 wt.% Bi. Similar results were obtained by other workers [6] for a series of alloys containing up to 0.55 wt.% Bi. In addition, pitting corrosion occurred in some grids with 0.1 wt.% Bi.

The inconsistent behaviour of lead–bismuth grids has prompted a number of corrosion studies using a variety of electrochemical techniques [7–17]. From measurements of the weight loss of lead–bismuth anodes in 1 M H_2SO_4 [10], it was reported that while the alloys were more susceptible to corrosion than lead itself, the stability rapidly decreased from pure lead to a minimum value at 3.5 wt.% Bi. Confirmation that the extent of the anodic attack is not a linear function of the bismuth content was later obtained [13, 14] from cyclic voltammetric and potential-step investigations of the formation/discharge of PbO_2 on lead–bismuth alloys in 5 M H_2SO_4. In that work, alloys with bismuth contents in the range 0.063 to 0.267 wt.% Bi were examined and it appeared that maximum stability was reached between 0.1 and 0.2 wt.% Bi. A further study [17] on a wider series of lead–bismuth alloys concluded that although small additions of bismuth may exert a protective effect on lead, the corrosion rate increases thereafter.

The grain structure of the alloy changes markedly with increasing additions of bismuth [18], and it has been shown [16] that there is an inverse relationship between grain size and corrosion rate. Thus, the diversities in corrosion behaviour reported by various workers may reflect differences in the physical structure of the alloys under investigation. Nevertheless, the mechanism by which bismuth accelerates grid corrosion has yet to be resolved.

In the work reported here, the technique of cyclic voltammetry has been used to compare the corrosion behaviour of both pure lead and a series of lead–bismuth alloys in 5 M H_2SO_4. In order to obtain readily measurable effects, this initial exploration of the phenomenon has been conducted on alloys containing significantly higher amounts of bismuth than those normally encountered in battery grids. The alloys have been subjected to grain refinement (through either bismuth addition or thermal treatment) in order to determine the extent to which grain boundaries contribute to the corrosion characteristics of the lead. The corresponding influence of bismuth when present in the electrolyte has also been examined.

Experimental

Alloy composition

A series of lead–bismuth alloys was obtained by casting 99.999 wt.% lead, alloyed with a given amount of bismuth, in split graphite moulds. The alloys contained 0.71, 1.42, 2.87 and 5.65 wt.% Bi, respectively.

Electrode preparation

To prepare working electrodes, the alloy specimens were pressed, either at room temperature or at −195 °C, to a thickness of 1 mm and then cut into 5×20 mm coupons. One coupon containing 5.65 wt.% Bi was annealed at 160 °C for 24 h and then quenched in water. The coupons were soldered to threaded brass mounts, encased in epoxy resin, and machined to expose a surface (area 0.1 cm^2) at a 45° angle in order to prevent entrapment of gas bubbles. The electrode assembly was screwed on to a stainless-steel rod that was sheathed in a glass tube. The latter was sealed at each end with Teflon stoppers.

The specimens were polished initially with 1200 grade silicon carbide paper. Scanning electron micrographs of these specimens, following cyclic voltammetric experiments (see below), revealed that imbedded polishing media caused discontinuities in the $PbSO_4$ film. These surfaces, as well as those of specimens polished with 2 μm magnesia, 1 μm diamond paste or tissue paper, possessed many surface irregularities due to the abrasive action of the polishing media. Chemical etching is an alternative procedure for surface preparation. Unfortunately, however, brief etching (5 s) of polished specimens in 10 wt.% nitric acid resulted in the formation of dark surface films. It was concluded, therefore, that pretreatment of surfaces by either mechanical polishing or chemical etching was inappropriate and would give rise to uncertainty in both the reproducibility and the nature of the surface films formed during subsequent experimentation. Consequently, the technique of electropolishing (after some mechanical polishing with 1200 grade silicon carbide paper) was adopted. Using a solution consisting of 90 g sodium acetate, 470 ml glacial acetic acid and 110 ml double-distilled water, electropolishing a current density of 1 A cm^{-2} (applied in pulses of 10 to 15 s) yielded a smooth surface with the grain boundaries clearly visible. Furthermore, the process removed any polishing particles that may have become imbedded in the specimens during the preliminary mechanical treatment. Prior to placement in the test cell, the electrodes were rinsed with double-distilled water and then dried successively with ethanol, acetone and air.

Experiments were performed in a glass cell consisting of working and counter electrode compartments separated by a glass frit, and a third compartment that housed the reference electrode. The counter electrode was a platinized-platinum foil electrode with an area of 1.3 cm^2. A Hg/Hg_2SO_4/ 5 M H_2SO_4 electrode was used as the reference electrode. All potentials are reported with respect to this electrode. The electrolyte was 5 M H_2SO_4

prepared from AR select reagent and double-distilled water. Investigations examining the effect of bismuth in solution on lead corrosion were performed in 5 M H_2SO_4 into which laboratory-grade bismuth sulphate had been dissolved.

The assembled cell was immersed in a water bath that was maintained at a temperature of 25 °C. At the conclusion of each experiment, the specimen was withdrawn and the surface area exposed to the electrolyte was measured with vernier calipers.

Cyclic voltammetry

Cyclic voltammetric studies were performed using a PAR model 273 potentiostat/galvanostat that was interfaced with an IBM personal computer equipped with PAR model 270 electrochemical software. A typical series of experiments for each specimen began with a 2 min cathodic treatment at −1.8 V to reduce any surface films. This was followed immediately by 10 'pre-conditioning' cycles over the range −1.8 to 1.7 V to form a reproducible surface. Finally, 5 cycles were applied between −1.8 and 1.25 V with a vertex delay of 180 s at 1.25 V. This delay and potential were required to give an anodic peak on the negative sweep at 1.1 V; the peak was not observed unless the previous negative scan had been taken into the region where $PbSO_4$ is reduced to lead. The formation of PbO_2 was restricted by limiting the potential of the positive-going scan to 1.25 V; otherwise, the cathodic current associated with the reduction of PbO_2 would partially, or totally, obscure the anodic peak at 1.1 V [19] For experiments using 99.999% Pb specimens in solutions of bismuth sulphate in 5 M H_2SO_4, the pre-conditioning cycles were followed by 20 cycles in the potential range −1.8 to 1.25 V with a vertex delay of 180 s at 1.25 V. All cycles were performed at a scan rate of 10 mV s^{-1}. During each experiment, high-purity nitrogen was bubbled slowly over the electrode in order to remove dissolved oxygen in the electrolyte and to displace small bubbles of hydrogen that tended to adhere to the electrode surface. The charges associated with the individual features of the cyclic voltammograms were calculated from the areas under expanded plots of the features. The areas were measured with a digital planimeter.

Grain boundary measurements

The lead and lead–bismuth alloy specimens were electropolished until the grain boundaries became visible, and then etched in a solution of two parts acetic acid, two parts nitric acid and five parts double-distilled water. The specimens were photographed under a Reichert optical microscope at a magnification of ×42. A grid of eight parallel lines, spaced 1 cm apart, was placed upon each photograph. The method of lineal analysis [20] was used to obtain the number of intersections of the grain boundaries in the specimen with the grid lines. This number is directly proportional to grain size. Two photographs, taken at different locations, were analyzed for each specimen. The mean number of grain boundaries was determined and used

to describe the physical state of the surface of the lead or lead–bismuth alloy.

Electron microscopy

A Jeol JSM 840A scanning electron microscope was used to examine and photograph the surfaces of the lead and the lead–bismuth alloy specimens. The latter were removed from the cell at 0.8 V, or during the positive and negative scans of cyclic voltammograms over the potential range −1.8 to 1.25 V. Specimens were gold coated using a Dynavac SC-150 sputter coater. Micrographs were obtained at magnifications between ×1500 and ×7000.

Results

Cyclic voltammetry

Cyclic voltammograms obtained in the potential range −1.8 to 1.25 V, with the potential held at 1.25 V for 180 s, exhibit five features that were used as a basis for comparing the behaviour of the lead and the lead–bismuth alloy specimens. Figure 1(a) presents these features for a lead specimen. Feature A (−890 mV, positive sweep) is due to the oxidation of lead to $PbSO_4$. Feature B (between −200 and 1250 mV, positive sweep, Fig. 1(b)) results from the oxidation of lead below the $PbSO_4$ layer to give a range of lead oxides and basic lead sulphates [21]. Feature C (1100 mV, negative sweep, Fig. 1(b)) is an anodic peak that arises from the corrosion of lead exposed during the discharge of PbO_2 [19]. Feature D (between −780 and −880 mV, negative sweep) is due to the reduction of lead oxides and basic lead sulphates to lead. Feature E (−1000 mV, negative sweep) is associated with the reduction of $PbSO_4$ to lead [22]. The latter feature also exhibits a second peak, or shoulder, that is independent of stirring and becomes less prominent when lead is alloyed with bismuth. This sub-feature has been observed by other workers [23].

The charge densities of features A and E for lead and different lead–bismuth alloys subjected to the same thermal treatment show (Table 1) that bismuth has little effect on the quantity of $PbSO_4$ that is formed. A similar result was obtained for lead cycled in 5 M H_2SO_4 solutions containing dissolved bismuth at a concentration above 0.535×10^{-4} M (Table 2). (note, a larger number of cycles was applied in the latter experiments and this probably accounts for the slightly different charge densities observed with the lead specimens (cf. values in Tables 1 and 2.))

The features of the cyclic voltammograms that appeared to be influenced most by bismuth were B, C and D. The charge densities of features B and D for lead and the various alloys pressed at 25 °C, as well as those for a specimen of lead pressed at −195 °C and a Pb–5.65wt.%Bi alloy annealed at 160 °C for 24 h, are given in Table 1. For alloys pressed at 25 °C, these charge densities appear to increase with increasing bismuth content. Low-temperature pressing of lead also yields an increase in charge density, but

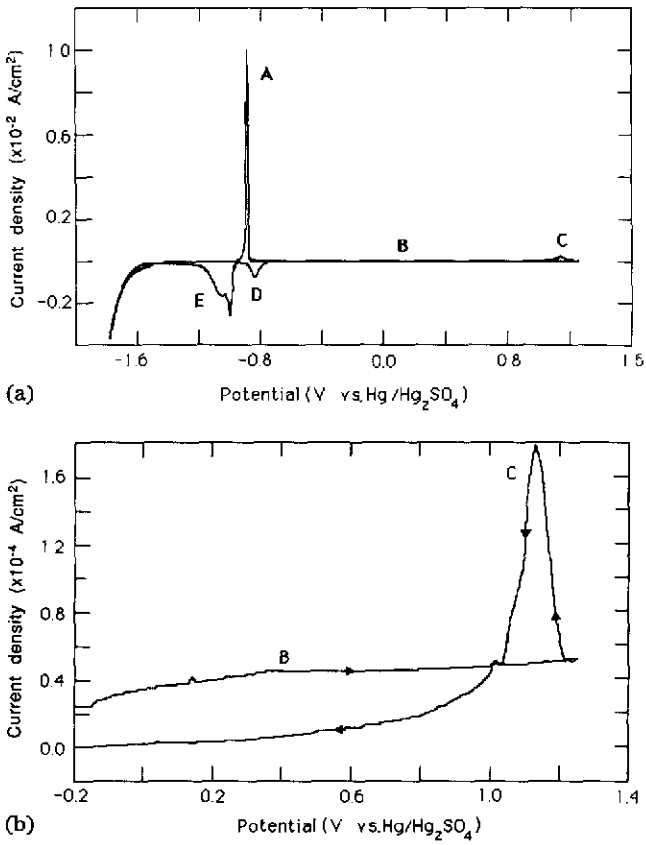

Fig. 1. (a) Typical cyclic voltammogram for 99.999% Pb cycled between −1.8 and 1.25 V at 10 mV s^{-1}; (b) expanded view of features B and C.

annealing of lead–bismuth alloy produces the reverse effect. The data presented in Fig. 2 show that the charge densities for features B and D exhibit an approximately linear dependence upon the number of grain boundaries. This suggests that the increase in charge results from bismuth causing grain refinement of the lead. The observed (Table 1) direct dependence of the number of grain boundaries on the charge density for differently treated lead and Pb–5.65wt.%Bi alloy specimens (see Fig. 3 for the effect of annealing on grain size) reinforces the conclusion that the physical structure of the alloy exerts an influence on features B and D.

In order to determine whether bismuth in solution also effects features B and D, a lead specimen was cycled in 5 M H_2SO_4 doped with Bi^{3+} ions in a range of concentrations from 0 to 4.5×10^{-4} M. It was found that the charge density of features B and D increases with increasing Bi^{3+} concentration up to 2×10^{-4} M (Table 2). Taken with the findings reported above, it can be concluded that both grain-size modification and bismuth ions in solution

TABLE 1

Cyclic voltammetric and structural features of pure lead and lead–bismuth alloys

Charge density	Alloy/thermal treatment						
	99.999 wt.% Pb		Pb–0.71wt.%Bi 25 °C pressed	Pb–1.42wt.%Bi 25 °C pressed	Pb–2.87wt.%Bi 25 °C pressed	Pb–5.65wt.%Bi	
	25 °C pressed	−195 °C pressed				25 °C pressed	160 °C annealed
Feature A (C cm^{-2})	0.0146	0.0427	0.0144	0.0124	0.0132	0.0125	0.0159
Feature B (C cm^{-2})	0.0061	0.0068	0.0076	0.0099	0.0090	0.0180	0.0100
Feature C (C cm^{-2})	0.0111	0.0119	0.0065	0.0036	0.0025	0.0011	0.0040
Feature D (C cm^{-2})	0.0056	0.0081	0.0073	0.0069	0.0082	0.0136	0.0079
Feature E (C cm^{-2})	0.0271	0.0393	0.0254	0.0276	0.0227	0.0287	0.0300
Mean number of grain boundaries	150	220	258	352	326	1058	157
Current density at 1.7 V (A cm^{-2})	0.0200	0.0178	0.0091	0.0070	0.0075	0.0058	0.0060

TABLE 2

Influence of dissolved bismuth on cyclic voltammetric features of pure lead pressed at 25 °C

Charge density	Bi^{3+} ($\times 10^{-4}$ M)				
	0	0.535	1.07	2.14	4.28
Feature A (C cm^{-2})	0.0159	0.0100	0.0092	0.0091	0.0780
Feature B (C cm^{-2})	0.0054	0.0090	0.0126	0.0137	0.0133
Feature D (C cm^{-2})	0.0046	0.0098	0.0097	0.0121	0.0123
Feature E (C cm^{-2})	0.0312	0.0251	0.0242	0.0259	0.0253

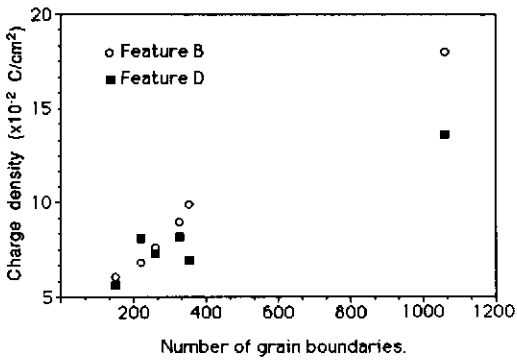

Fig. 2. Charge density vs. number of grain boundaries for features B and D from lead–bismuth alloys.

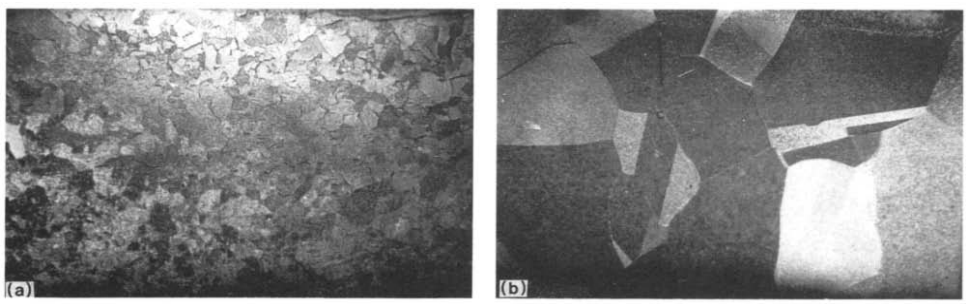

Fig. 3. Optical micrographs of an electropolished and etched Pb–5.65wt.%Bi alloy: (a) pressed at room temperature; (b) pressed at room temperature and annealed at 160 °C for 24 h.

influence the corrosion of lead under the $PbSO_4$ layer (feature B), as well as the reduction of the subsequent products to lead (feature D).

When bismuth is present in either the alloy or the electrolyte, feature D may not consist of a single peak (Figs. 4 and 5). In addition, feature D is shifted to potentials more negative than the single peak observed at −840 mV with a 99.999 wt.% Pb specimen. The fine structure of feature D is

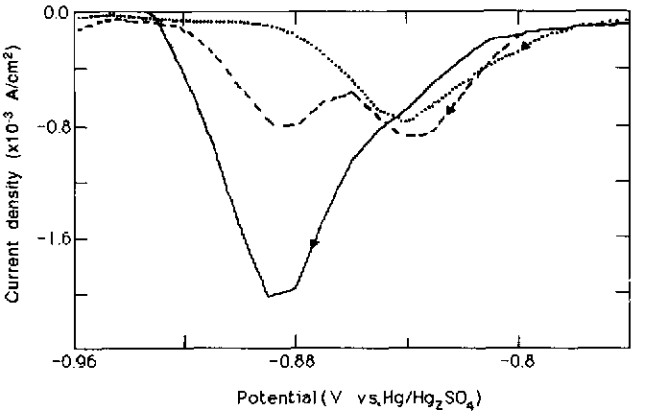

Fig. 4. Influence on feature D of alloy composition for scans between −1.8 and 1.25 V: (·····) 99.999 wt.% Pb; (– – –) Pb–1.42wt.%Bi; (——) Pb–5.65wt.%Bi.

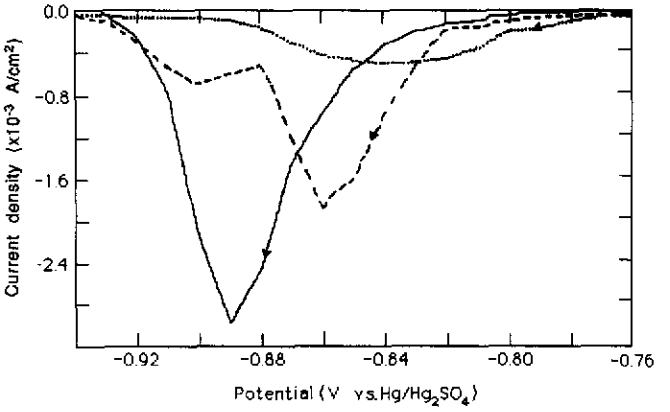

Fig. 5. Influence on feature D of Bi^{3+} concentration in the electrolyte for scans between −1.8 and 1.25 V. Bi^{3+} concentration: (·····) 0 M; (– – –) 1.07×10^{-4} M; (——) 4.28×10^{-4} M.

extremely difficult to reproduce and depends markedly upon the electrode pretreatment and charge/discharge history.

The dependence of the charge density for feature C on bismuth content is given in Table 1. It can be seen that feature C decreases with increasing bismuth concentration. This could arise either from a real decrease in anodic current (i.e., from reduced corrosion of the substrate), or from a real increase in the overlapping cathodic current due to PbO_2 discharge causing an apparent decrease in anodic current. Measurements of the current density at 1.7 V on positive scans over the potential range −1.8 to 1.7 V show (Table 1) that PbO_2 formation is inhibited by the presence of bismuth. Consequently, the observed behaviour of feature C cannot be due to an increase in overlapping cathodic current and must, therefore, arise from a decrease in the corrosion of lead below the discharging PbO_2.

Discussion

Cyclic voltammetry

Discussion is limited to features B, C and D of the cyclic voltammograms as the above investigations show that these are particularly sensitive to the presence of bismuth.

Feature C

Sharpe [19] has claimed that feature C results from corrosion of the substrate residing below the layer of discharging PbO_2. Other workers argue [24] that stresses, induced by differences in the molar volumes of PbO_2 and $PbSO_4$, cause cracks to form in the surface layers and that these, in turn, expose the underlying lead to further corrosion. Indeed, stress cracking of the corrosion layer surrounding battery grids is extremely common [25]. The observed decrease in anodic current for feature C with increasing bismuth content, in both alloys and doped electrolytes, indicates that the corrosion product formed on lead during the positive sweep in the presence of bismuth is more resistant to the internal stresses imposed by molar volume changes. Hence, fewer cracks are formed. This observation may provide the basis for an explanation of the observed [4, 5] influence of bismuth on the growth of battery grids.

Features B and D

Extensive investigations [21, 26, 27] of the corrosion products on lead in the potential region of feature B have shown that, between −300 and 900 mV, the following compounds form below the $PbSO_4$ layer (which develops up to −300 mV): PbO, $5PbO \cdot 2H_2O$, $PbO \cdot PbSO_4$ and $3PbO \cdot PbSO_4 \cdot H_2O$. These compounds are only stable in an alkaline environment. A mechanism for the development of such an environment has been proposed [27–29]. In this, it is assumed that $PbSO_4$ crystals hinder the diffusion of SO_4^{2-} ions towards the lead surface. This, in turn, allows lead to corrode via dissociation of H_2O, diffusion of H^+ and OH^- ions, and precipitation of basic sulphates. The pH below the $PbSO_4$ film will, therefore, depend on the porosity of the film. The observed increase in the charge density for feature B (and, consequently, for feature D) with increasing bismuth content suggests that bismuth modifies the nature of the $PbSO_4$ layer and, thereby, the pH of the solution in the region below.

Effect of $PbSO_4$ morphology

Scanning electron microscopy confirmed that bismuth, either as an alloy or dissolved in the acid, affects the morphology of the $PbSO_4$ layer (Fig. 6). Pure lead shows a flat surface of finely grained (0.5 μm) $PbSO_4$. The grain size is similar when bismuth is present but the crystals appear to form aggregates that give rise to a surface of greater roughness and, therefore, greater porosity. These findings are in agreement with other published work

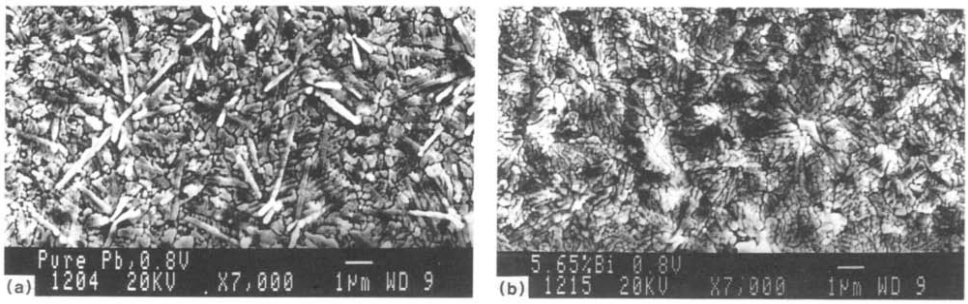

Fig. 6. Electron micrographs of (a) 99.999% Pb and (b) Pb–5.65wt.%Bi specimens at 800 mV on a positive sweep. Magnification bar = 1 μm.

[30] that found the $PbSO_4$ film on a Pb–0.57wt.%Bi alloy to contain a greater range of crystal sizes than the film formed on pure lead.

As with pure lead, the consumption of sulphate, together with the inherent property of $PbSO_4$ in restricting acid diffusion, favours an increase in pH in the region below and, hence, facilitates the formation of lead oxides and basic lead sulphates. Furthermore, since the $PbSO_4$ layer is more porous in the presence of bismuth, there is enhanced attack of the substrate and greater amounts of corrosion products are formed, as witnessed by the increase in the charge densities associated with features B and D (Table 1). It is possible that the thicker corrosion layer formed on lead–bismuth alloys provides added protection to the substrate during reduction of PbO_2 to $PbSO_4$ and may, therefore, contribute in part to the observed decrease in feature C.

Effect of grain boundaries

Figure 2 shows that there is a direct correlation between the incidence of grain boundaries and the amount of lead oxides and basic lead sulphates formed under the $PbSO_4$ film. This suggests that the compounds are produced preferentially along the grain boundaries. The grain size can be influenced by the addition of bismuth as an alloying agent or by thermal treatment of the specimen (Table 1).

Conclusions

The above studies show that alloys containing > 0.7 wt.% Bi influence the corrosion of lead in 5 M H_2SO_4, both through modification of the physical structure of the alloy itself and through changes in the morphology and quantity of the corrosion product. While the adverse effects of increasing bismuth content on grain size can be moderated through heat treatment of the alloy, the overall corrosive attack beneath the $PbSO_4$ layer is still greater than that experienced by pure lead.

Acknowledgement

The authors are grateful to Dr M. S. J. Gani of the Department of Materials Engineering, Monash University, for supplying the lead–bismuth alloys used in this investigation.

References

1 G. L. Corino, R. J. Hill, A. M. Jessel, D. A. J. Rand and J. A. Wunderlich, *J. Power Sources, 16* (1985) 141.
2 B. Agruss, E. H. Herrmann and F. B. Finan, *J. Electrochem. Soc., 104* (1957) 204.
3 J. L. Devitt and M. Myers, *J. Electrochem. Soc., 123* (1976) 1769.
4 E. Hoehne, *Metallwirtsch., 23* (1944) 60.
5 E. Hoehne, *Arch. Metallkd., 2* (1948) 311.
6 K. W. Grosheim-Krisco, K. W. Hanemann and W. Hofmann, *Z. Metallkd., 34* (1942) 97.
7 V. P. Moshovets and A. Z. Lyandres, *Zh. Prikl. Khim., 20* (1947) 347; *21* (1948) 441.
8 M. A. Dasoyan, *Dokl. Akad. Nauk. SSSR, 107* (1956) 863.
9 G. Bacsky, *Int. Symp. Anti Corrosion Protection, Bratislava, 1962.*
10 V. I. Bryntseva, V. G. Bundzhe, Yu. D. Dunaev, G. Z. Kiryakov and L. A. Tskhe, *Zashch. Met., 3* (1967) 504.
11 J. A. Gonzales, J. J. Royuela and S. Feliu, *Lead 68, Proc. 3rd Int. Conf., 1968,* Pergamon, Oxford, 1969.
12 J. A. Gonzales, J. J. Royuela and S. Feliu, *Rev. Metal. (Madrid), 7* (1971) 105.
13 N. A. Hampson, S. Kelly and K. Peters, *J. Electrochem. Soc., 127* (1980) 1456.
14 S. Kelly, N. A. Hampson and K. Peters, *J. Appl. Electrochem., 12* (1982) 81.
15 S. R. Ellis, M. Johnson, M. P. J. Brennan and N. A. Hampson, *Surf. Technol., 26* (1985) 11.
16 N. Papageorgiou, M. Skyllas-Kazacos and D. A. J. Rand, in T. Tran and M. Skyllas-Kazacos (eds.), *Electrochemistry: Current and Potential Applications, Proc. 7th Australian Electrochemistry Conf. (7AEC), Sydney, Australia, Feb. 15–19, 1988,* RACI, Melbourne, 1988, pp. 32–35.
17 S. Webster, P. J. Mitchell, N. A. Hampson and J. Dyson, *Inst. Chem. Eng. Symp. Ser., 98* (1986) 217.
18 M. Johnson, S. R. Ellis, N. A. Hampson, F. Wilkinson and M. C. Ball, *J. Power Sources, 22* (1988) 11.
19 T. F. Sharpe, *J. Electrochem. Soc., 122* (1975) 845.
20 R. C. Gifkins, *Optical Microscopy of Metals,* Pitman, London, 1970, p. 182.
21 D. Pavlov, C. N. Poulieff, E. Klaja and N. Iordanov, *J. Electrochem. Soc., 116* (1969) 316.
22 H. S. Panesar, in D. H. Collins (ed.), *Power Sources 3,* Oriel, Newcastle upon Tyne, 1971, pp. 79–89.
23 T. G. Chang, M. M. Wright and E. M. L. Valeriote, in D. H. Collins (ed.), *Power Sources 6,* Oriel, Newcastle upon Tyne, 1977, pp. 69–89.
24 R. L. Deutscher, S. Fletcher and J. A. Hamilton, *Electrochim. Acta, 31* (1986) 585.
25 A. M. Hardman, R. T. Hopwood, J. E. Manders, D. A. J. Rand, J. Reitz and H. Tuphorn, *J. Power Sources, 23* (1988) 257.
26 D. Pavlov and N. Iordanov, *J. Electrochem. Soc., 117* (1970) 1103.
27 D. Pavlov and R. Popova, *Electrochim. Acta, 15* (1970) 1483.
28 P. Reutschi, *J. Electrochem. Soc., 120* (1973) 331.
29 E. M. L. Valeriote and L. D. Gallop, *J. Electrochem. Soc., 124* (1977) 370.
30 D. M. Rice, *J. Power Sources, 28* (1989) 69.